Temperature effect on domain-wall damping in an amorphous alloy

Claudio Aroca and Eloísa López
Laboratorio de Magnetismo, Facultad de Ciencias Físicas, Universidad Complutense, Madrid 3, Spain

Pedro Sánchez
Departamento de Física, E.T.S. Ingenieros Telecommunicación, Universidad Politécnica, 28040 Madrid, Spain and Departamento de Física, Universidad Politécnica, Madrid 3, Spain

(Received 7 November 1983; revised manuscript received 8 May 1984)

The temperature dependence of the viscous damping parameter β, restoring constant α, and propagation field H_p have been measured in ferromagnetic amorphous ribbons. We have observed that there is a linear dependence of β on $(\mu_0 M_s)^2/\rho$ up to $T=0.9T_c$ and that α is proportional to $(\mu_0 M_s)^2$. From these data, it is possible to estimate the eddy-current (β_E) and relaxation (β_R) contributions to β separately. It is further inferred that the number of domain walls and the magnetic pole distribution in the sample do not change up to $T \simeq 0.9T_c$.

INTRODUCTION

Domain-wall motion, under an external field, is controlled by the parameters α and β. The viscous damping parameter β is due to eddy-current and relaxation effects, the observed β being the sum $\beta=\beta_E+\beta_R$. The restoring constant α is related to the potential-energy minimum in which the wall is located, and two terms must be considered: α_N, due to magnetostatic energy, and α_D due to crystal imperfections such as microstresses or inclusions.[1]

Samples with simple domain structures are suitable for obtaining micromagnetic information. Single crystals and amorphous alloys meet this requirement, and have been studied extensively under various experimental configurations.[2–8]

We have studied Bloch wall motion in $Fe_{40}Ni_{40}P_{14}B_6$ (Metglas 2826) amorphous ribbons, since its high resistivity ($\rho=1.66\times10^{-6}$ Ω m),[9] and its thickness ($e=45$ μm) make both kinds of damping effective. Some authors have obtained data from measurements on Metglas 2826, but have disagreed about the relative values of β_E and β_R. For example, O'Handley[10] has obtained $\beta=5$ kg m^{-2}s^{-1} and $\beta_E/\beta_R \simeq 1$, while Williams and Bishop,[6] and Eifrig, Grosse-Nobis, and Jansen[7] have obtained $\beta_E \simeq 12.6$ kg m^{-2}s^{-1} and $\beta_R \simeq 3$ kg m^{-2}s^{-1}.

In this work, we have used an experimental procedure that enables us to measure the dependence of the parameters β and α on temperature. From these measurements, β_E and β_R are estimated separately, avoiding the generally used method of subtracting the evaluated eddy-current damping $\beta_E=C\,(\mu_0 M_s)^2/\rho$ (Refs. 1 and 2) from the measured parameter β in order to arrive at a value for β_R. The calculation of β_E is not easy because the constant C depends on the shape of the propagating domain wall. From our measurements, C can be evaluated experimentally.

EXPERIMENTAL METHODS

The equation of motion for a 180° domain wall, under the action of an ac magnetic field of amplitude H_2 and frequency $(\omega/2\pi)$, is

$$\beta\frac{dx}{dt}+\alpha x=2\mu_0 M_s H_2 \sin(\omega t)\ ,$$

where the wall mass is neglected. Assuming that α does not depend on t or x, the emf $\mathscr{E}=\mathscr{E}_0\cos(\omega t-\phi)$ induced by domain-wall motion in a sense coil with n turns is

$$\mathscr{E}=\frac{4n(\mu_0 M_s)^2 H_2 e\omega}{(\alpha^2+\beta^2\omega^2)^{1/2}}\cos(\omega t-\phi)\ . \tag{1}$$

We have obtained α and β by measuring $\mathscr{E}_0$ as a function of H_2 and ω, at different temperatures.

Measurements were made on 6- and 8-cm-long samples of $Fe_{40}Ni_{40}P_{14}B_6$ amorphous ribbons. To reduce perpendicular anisotropy and to get an almost homogeneous anisotropy in the ribbon, the samples were preannealed at 300 °C for 1.5 h and cooled at 5 °C/min rate. We ensured that α does not depend on x or t by using samples short enough to get $\alpha_N >> \alpha_D(x,t)$. The demagnetizing factor in amorphous ribbons is $N=8.0\times10^{-2}(l/d)^{-1.75}$,[11] where l and d are the length and width of the sample, respectively. With a saturation magnetization $(\mu_0 M_s)=0.7$ T, $d=1.2$ mm, $l_A=6$ cm, and $l_B=8$ cm, the demagnetizing field in the saturated samples are calculated as $H_{N(A)}=47.6$ A m^{-1} and $H_{N(B)}=28.6$ A m^{-1}, respectively. Since α_D is related to the coercive field ($H_c=1$ A m^{-1}) and α_N is related to H_N, $\alpha_N >> \alpha_D$ is expected.

Each sample, surrounded by the sense coil, was placed in a silicon oil bath to avoid oxidation during heating. Due to the short sample lengths used, it was easy to get a uniform temperature. A 200-MPa tensile stress was applied to the samples in order to get a longitudinal domain wall.[6,12,13]

A system of Helmholtz coils provided a magnetic field $H=H_1+H_2$, with $H_1 \simeq H_N$ at a frequency $f_1=0.1$ Hz; the amplitude of H_2 ranged from 0 to 1.9 A m^{-1}, and its frequency $\omega/(2\pi)$ from 20 to 6000 Hz. In this way, the domain wall is being "shaken" by an ac field, while it is displaced very slowly, from one edge of the sample to the other. The H_2 field amplitude is not high enough to nucleate other walls.

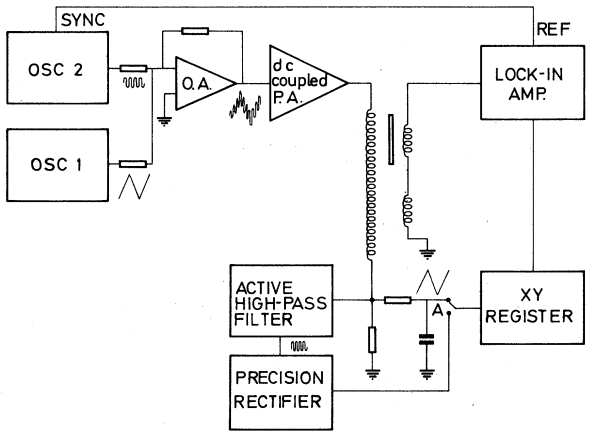

FIG. 1. Block diagram of the experimental setup.

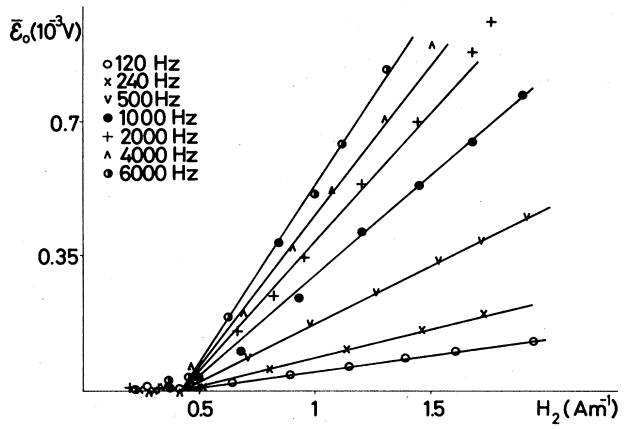

FIG. 3. $(\bar{\mathcal{E}}_0, H_2)_\omega$ curves at $T=80\,^\circ\mathrm{C}$ ($l=6$ cm, $n=156$).

The emf $\mathcal{E}$, induced by wall shaking, is measured using a lock-in amplifier, locked with the field H_2. By switching A, we can plot the lock-in output $\mathcal{E}_0$ vs H_1 or H_2, in the XY register (Fig. 1).

Figure 2 shows the output $\mathcal{E}_0$ vs H_1. At $|H_1| < |H_N|$, the induced emf is nearly constant, except for fluctuations related to α_D. Measurements were made by choosing a lock-in time constant greater than $1/f_1$. In this way, the mean value of $\mathcal{E}_0$ when H_1 was changing from $-H_N$ to $+H_N$, $(\bar{\mathcal{E}}_0)$ is obtained, for a constant value of H_2. For different values of H_2 and ω, curves similar to Fig. 3 were obtained.

$\bar{\alpha}$ and $\bar{\beta}$, the respective average values of the parameters α and β, can be determined from these curves. In our method, $\bar{\alpha}=\alpha_N$. At low frequencies, $\mathcal{E}_0$ is related to $\bar{\alpha}$ by $\bar{\mathcal{E}}_0=4n(\mu_0 M_s)^2 H_2 e\omega/\bar{\alpha}$; and at high frequencies, $\bar{\beta}$ is determined from $\bar{\mathcal{E}}_0=4n(\mu_0 M_s)^2 H_2 e/\bar{\beta}$ [see Eq. (1)].

Figure 3 is a plot of $\mathcal{E}_0$ vs H_2. In all the curves in this figure, experimental points can be fitted to straight lines that intercept the H_2 axis at H_p. The discrepancy between experimental results and Eq. (1) is due to the assumption in Eq. (1) that the domain wall will displace at any field. As is well known, a domain wall does not move under an external field until it reaches a critical value known as the propagation field H_p. Therefore, the $\mathcal{E}_0$ value of Eq. (1) must be rewritten as

$$\mathcal{E}_0=\frac{4n(\mu_0 M_s)^2(H_2-H_p)e\omega}{(\alpha^2+\beta^2\omega^2)^{1/2}} .$$

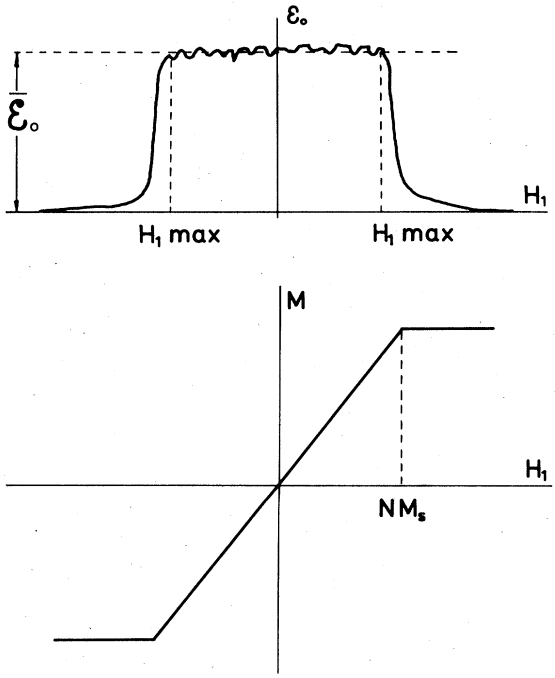

FIG. 2. (a) $\mathcal{E}_0$ vs H_1 (experimental curve). The $\bar{\mathcal{E}}_0$ value is indicated. (b) Schematic hysteresis loop.

RESULTS AND DISCUSSION

Curves like Fig. 3 have been obtained for 8- and 6-cm-long samples in a temperature range from 25 to 230 °C. From them, we get that the H_p value decreases linearly with temperature (Fig. 4) from 0.6 A m^{-1} at 25 °C to 0.1 A m^{-1} at 230 °C. The H_p temperature dependence can be explained on the basis that the thermal agitation effect is simi-

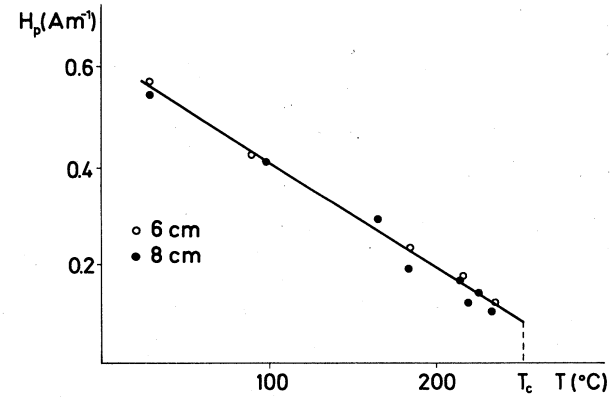

FIG. 4. Temperature influence on the propagation field H_p.

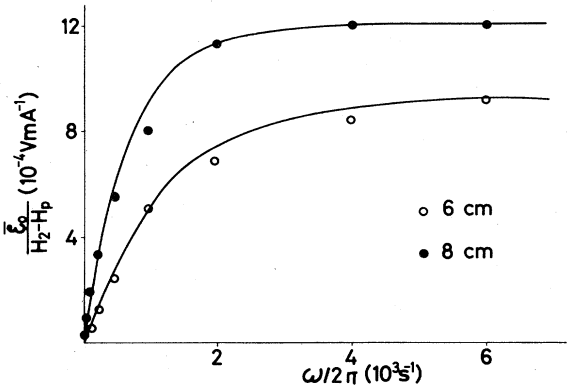

FIG. 5. Theoretical curves (solid lines) and experimental points (circles): $\bar{\mathscr{E}}_0/(H_2-H_p)$ vs $\omega/2\pi$ (●: $l=8$ cm, $n=191$; ○: $l=6$ cm, $n=156$).

lar to a random high-frequency ac field which, when added to the applied field, makes domain-wall propagation easier.[3]

The slopes $\bar{\mathscr{E}}_0/(H_2-H_p)$ of the straight lines of Fig. 3 were plotted versus ω, obtaining the data points in Fig. 5. These data enable us to get the average values of α and β for the sample $(\bar{\alpha},\bar{\beta})$ by best fitting theoretical curves into experimental points.

The parameter α_N due to magnetostatic energy, is related to the demagnetizing factor N by the expression

$$\alpha_N=\frac{4\mu_0 M_s^2 N}{d}.$$

There is the good agreement (Fig. 6) between α_N vs $(\mu_0 M_s)^2$, calculated from the expression above and our experimental results $\bar{\alpha}$ vs $(\mu_0 M_s)^2$ for 6- and 8-cm-long samples. Discrepancies between the theory and the experiment can be attributed to errors in empirical expression of N.[11]

As mentioned earlier, the eddy-current contribution β_E to damping parameter β is given by $\beta_E=C(\mu_0 M_s)^2/\rho$. Measurements were made of $M_s(T)$ and $\rho(T)$ from $T=25\,^\circ$C to $T=T_c=245\,^\circ$C, and by plotting experimental $\bar{\beta}$ values

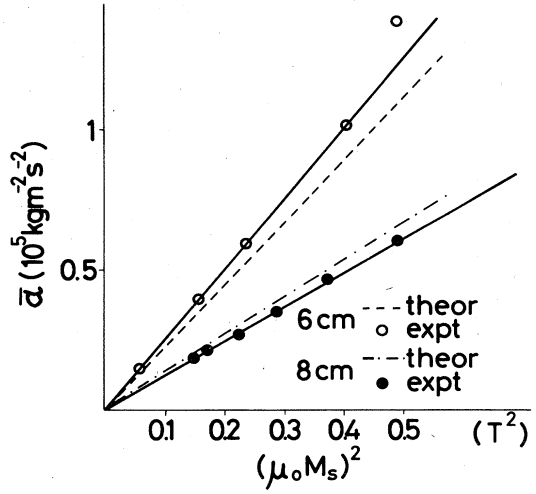

FIG. 6. Theoretical α_N and experimental $\bar{\alpha}$ vs $(\mu_0 M_s)^2$.

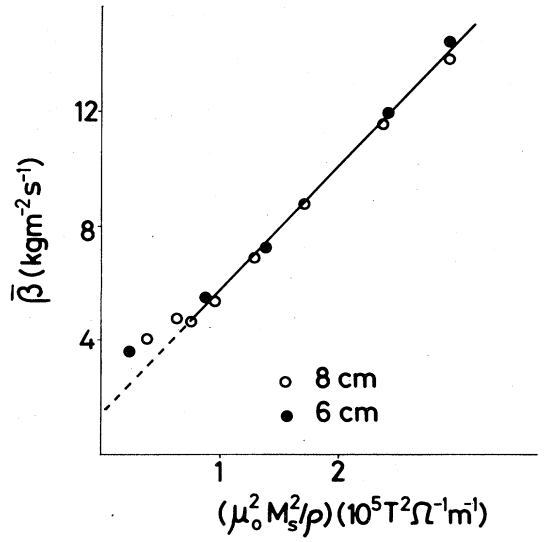

FIG. 7. Experimental values of $\bar{\beta}$ at various temperatures vs corresponding $(\mu_0 M_s)^2/\rho$ for 6- and 8-cm-long samples.

versus $(\mu_0 M_s)^2/\rho$, Fig. 7 was obtained. At temperatures below 220 °C ($\mu_0 M_s=0.38$ T and $\rho=1.77\,\mu\Omega$ m) experimental values of $\bar{\beta}$ can be fitted by a straight line that intercepts the $\bar{\beta}$ axis at $\bar{\beta}=1.4$ kg m^{-2}s^{-1}, which is interpreted as $\beta_R=\bar{\beta}(T)-\beta_E(T)$.

The origin of relaxation damping should be the same as that of the precession motion on magnetization. Formally, it can be expressed for materials with very large resistivity as shown by Kittel:[14]

$$\beta_R=8\pi^2\mu_0\lambda/(\nu^2\delta)\ ,$$

where λ is the relaxation frequency which appears in the Landay-Lifshitz equation, ν the gyromagnetic constant, and δ the domain-wall thickness. As the experimental data of $\bar{\beta}$ can be fitted by straight lines and $\bar{\beta}=C(\mu_0 M_s)^2/\rho+\beta_R$ it can be inferred that β_R is constant up to $T=220\,^\circ$C ($\sim 0.90\,T_c$), which then seems to be consistent with results for crystalline materials.[15]

From these results and $\delta=1.5\times10^{-7}$ m,[16] a value of $(\lambda/\nu^2)=2.1\times10^{-3}$ m^{-2}A^{2}s can be evaluated. This value is larger than those for crystalline materials,[17] due probably to the larger thickness of the domain wall in amorphous materials.

Over 220 °C, the error of our experimental procedure increases, because α_N depends on $(\mu_0 M_s)^2$, and $\alpha_D(x,t)$ is not negligible anymore, versus α_N. It would be interesting to obtain more precise measurements over 220 °C up to T_c, by using shorter samples.

CONCLUSIONS

The damping parameter β has been measured at different temperatures, from 25 to 230 °C, in Metglas 2826 ribbons under sufficient tension to render it effectively uniaxial. From these measurements we have obtained precise values of both kinds of damping parameters: β_E and β_R. At room temperature we get $\beta_E=12.8$ kg m^{-2}s^{-1} and $\beta_R=1.4$ kg m^{-2}s^{-1}, values which are in good agreement with those obtained by a quite different method.[6] From mea-

surements of β at different temperatures, it has been deduced that the constant C in $\beta_E = C(\mu_0 M_s)^2/\rho$ is not temperature dependent, which implies that the shape of the propagating domain wall does not change appreciably when temperature increases up to $T \simeq T_c$.

The experimental value of C obtained by us, $C = 0.96e$ where $e = 45\ \mu$m, is higher than the theoretical value obtained for a simple domain wall $C = 0.54e$ in Ref. 2. This can be due to the fact that in the theoretical calculation of C, the domain-wall thickness was neglected. Besides, roughness of the ribbon affects the evaluation of $\mu_0 M_s$, and thus also affects the obtained value for the constant C.

The propagation field H_p has been measured and we have found it to decrease linearly with increasing temperature..

ACKNOWLEDGMENTS

We gratefully acknowledge valuable discussions with Dr. S. Velayos and Dr. A. Hernando.

[1]B. D. Cullity, *Introduction to Magnetic Materials* (Addison-Wesley, Reading, MA, 1972), p. 446.
[2]H. J. Williams, W. Shockley, and C. Kittel, Phys. Rev. **80**, 1090 (1950).
[3]R. Vergne, J. C. Cotillard, and J. L. Porteseil, Rev. Phys. Appl. **16**, 449 (1981).
[4]W. Grosse-Nobis and W. Shonfelder, Physica B **80**, 407 (1975).
[5]W. Grosse-Nobis, paper No. 26-7 presented at the INTERMAG Conference, Grenoble, 1981 (unpublished).
[6]P. Williams and J. E. L. Bishop, J. Magn. Magn. Mater. **20**, 245 (1980).
[7]H. Eifrig, W. Gross-Nobis, and K. Jansen, J. Magn. Magn. Mater. **6**, 73 (1977).
[8]J. M. Barandiarán and A. Hernando, Phys. Status Solidi (a) **61**, K107 (1980).
[9]K. Jansen, W. Grosse-Nobis, and H. Kleibink, J. Magn. Magn. Mater. **26**, 267 (1982).
[10]R. C. O'Handley, J. Appl. Phys. **46**, 4996 (1975).
[11]P. Sánchez, C. Aroca, and E. López, Ann. Fis. (B) **80**, 22 (1984).
[12]A. Hernando and J. M. Barandiarán, Phys. Rev. B **22**, 2445 (1980).
[13]C. Aroca, E. López, and P. Sánchez, J. Magn. Magn. Mater. **23**, 193 (1981).
[14]C. Kittel, Phys. Rev. **80**, 918 (1950).
[15]A. Aharoni, J. Appl. Phys. **53**, 11 (1982).
[16]E. López, C. Aroca, and P. Sánchez, J. Magn. Magn. Mater. **36**, 175 (1983).
[17]S. Chikazumi, *Physics of Magnetism* (Krieger, Huntington, NY, 1978).